

Brief Reports

Brief Reports are accounts of completed research which, while meeting the usual Physical Review standards of scientific quality, do not warrant regular articles. A Brief Report may be no longer than four printed pages and must be accompanied by an abstract. The same publication schedule as for regular articles is followed, and page proofs are sent to authors.

Phase diagram of betaine calcium chloride dihydrate in an applied electric field

Ian Folkins and M. B. Walker

Department of Physics, University of Toronto, Toronto, Ontario, Canada M5S 1A7

Z. Y. Chen

Xerox Research Centre of Canada, 2660 Speakman Drive, Mississauga, Ontario, Canada L5K 2L1

(Received 2 January 1991; revised manuscript received 11 March 1991)

The molecular crystal betaine calcium chloride dihydrate (BCCD) exhibits the largest number of structurally incommensurate and commensurate phases yet found. A model recently introduced by two of us reproduced the sequence and temperature stability interval of the commensurate phases, as well as the complex temperature dependence of the spontaneous polarization. We generalize the free energy of this model to include the effect of an applied electric field. The phase diagram of BCCD in an applied field is then calculated and the result compared with experiments.

The molecular crystal betaine calcium chloride dihydrate (BCCD) exhibits the largest number of structurally incommensurate and commensurate phases yet found. The magnitude $\alpha(T)$ of its modulation wave vector $\mathbf{k} = \alpha(T)\mathbf{c}^*$ decreases from slightly below $\frac{1}{3}$ at the initial 164-K normal-to-incommensurate transition to, successively, $\frac{3}{10}$, $\frac{2}{7}$, $\frac{5}{18}$, $\frac{3}{11}$, $\frac{7}{26}$, $\frac{4}{15}$, $\frac{6}{23}$, $\frac{1}{4}$, $\frac{2}{9}$, $\frac{1}{5}$, $\frac{2}{11}$, $\frac{1}{6}$, $\frac{2}{13}$, $\frac{1}{7}$, $\frac{1}{8}$ and finally zero at 46.0 K.¹ The region of temperature for which many of the commensurate phases are stable is too narrow to be measured by x-ray diffraction.² In these cases, the evidence for their existence comes principally from dielectric anomalies.^{1,3} These measurements also indicate that there are several intervals between the commensurate phases where the wave vector appears to vary continuously.

The "devil's staircase" behavior in the wave-vector magnitude, and the associated complex temperature dependence of the spontaneous polarization and dielectric constant, have motivated several mean-field models.³⁻⁷ One of these,⁴ recently introduced by two of us, successfully explained the wave-vector sequence, reproduced the observed spontaneous polarization and was able to predict space-group symmetries for the various phases. This paper generalizes the free energy of this model to nonzero applied electric fields. Doing this enables us to calculate the temperature versus applied electric-field phase diagram, and to compare the result with what is known about this diagram from experiment.

The normal-state crystal structure⁸ of BCCD contains four BCCD molecules within its orthorhombic unit cell. We envisage this structure as being composed of layers perpendicular to the c axis.⁴ The layers are not identical, however, as the c -axis periodicity is twice the interlayer

spacing. The soft mode responsible for driving the normal-to-incommensurate transition, and presumably the subsequent transitions at lower temperatures as well, is known⁹ to be of Λ_3 symmetry. The approach of Ref. 4 examines the displacements of the atoms in a particular layer caused by this mode. The wave vector of the Λ_3 mode is perpendicular to the layers. Hence, the relative displacements of any two ions in the same layer is prescribed by the polarization vector of the Λ_3 mode. In general, these displacements will not transform according to any single irreducible representation (IRREP) of the two-dimensional space group of a layer. They can, however, be split into two parts, one part transforming according to the Γ_2 two-dimensional IRREP and the other to the Γ_3 IRREP. The amplitude on layer l of the first part is referred to as v_l , the amplitude of the second as w_l . Symmetry prescribes to some extent what the ion displacements in the v_l and w_l symmetry modes are. For example, the two symmetry-related calcium ions of the two-dimensional unit-cell move in opposite directions along the b axis for v_l , but in the same direction for w_l .⁴

The ratio between v_l and w_l is independent of l for a particular Λ_3 mode. One can, however, relax this constraint to consider more general displacements from the normal state. The Landau model of Ref. 4 considers all v_l and w_l to be independent variables. The free energy of an isolated layer l is expanded to fourth order in powers of v_l and w_l . The two-dimensional symmetry of a layer will determine the form of this expansion. Interlayer interactions are represented by products of v_l and w_l with v_{l+1} and w_{l+1} . The form of these nearest-neighbor layer coupling terms will depend on the full three-dimensional

space group of BCCD. The resulting free energy can be shown⁴ to be,

$$F_0 = \sum_l \left(\frac{1}{2} a v_l^2 + \frac{1}{4} v_l^4 + \frac{1}{2} a' w_l^2 + \frac{1}{4} w_l^4 + \frac{1}{2} b v_l^2 w_l^2 \right) + \frac{1}{2} \sum_l (J v_l v_{l+1} + J' w_l w_{l+1}) + \frac{1}{2} \sum_l (v_l w_{l+1} - v_{l+1} w_l). \quad (1)$$

It should be valid as long as the displacements of a layer are small and the interactions between layers short ranged. The interlayer interaction terms will prescribe the variation in v_l and w_l as one goes from layer to layer. It is the competition between these terms that gives rise to the sensitive dependence of the modulation wave vector on changes in the parameters J and J' . Instead of using the parameters of Eq. (1), however, the authors of Ref. 4 introduce the parameters $a_{\pm} = \frac{1}{2}(a \pm a')$, $J_{\pm} = \frac{1}{2}(J \pm J')$, and b . They fix $a_- = 0.4$, $J_- = 0$, $b = 3$ and calculate the a_+ versus J_+ phase diagram. Their result is shown as Fig. 1. The trajectory $a_+ = 0.8J_+ + 1.6$ reproduces not only the succession of commensurate phases observed, but also their approximate temperature intervals, assuming J_+ varies linearly with temperature.

The free energy of Eq. (1) is expanded in terms of the displacements alone. An electric field applied to the crystal, however, will not interact with the displacements directly but rather through the crystal's polarization. Hence, to consider the effect of an electric field on BCCD, it is necessary to first couple the displacements with the polarization, and then the polarization with the field. The electric fields applied to BCCD and the average polarizations per layer of BCCD along the a and b directions will be referred to as E_a, P_a , and E_b, P_b , respectively. They will transform as vector components while the transformation properties of v_l and w_l are given in Ref. 4. These symmetries will dictate the lowest-order couplings between the displacements and polarization,

and polarization and field. They are,

$$F_e = \frac{m}{2} \chi_{0a}^{-1} P_a^2 + \frac{m}{2} \chi_{0b}^{-1} P_b^2 - m P_a E_a - m P_b E_b + c_{a1} P_a \sum_l (-1)^l v_l (w_{l+1} - w_{l-1}) + c_{a2} P_a \sum_l (-1)^l v_l^2 + c_{a3} P_a \sum_l (-1)^l w_l^2 + c_b P_b \sum_l w_l, \quad (2)$$

where m is the number of layers. Note that the displacements interact linearly with P_b but quadratically with P_a . This accounts for the relative weakness of the spontaneous P_a as compared to spontaneous P_b seen in experiments.

At equilibrium, the free energy F_e must be a minimum with respect to P_a and P_b . This condition can be used to solve for the polarizations in terms of the displacements and applied fields. The resulting expression for P_a involves four terms—a term linear in E_a , and the c_{a1} , c_{a2} , and c_{a3} terms quadratic in the displacements. The last three terms were discussed in Ref. 4, where it was found that each made a similar contribution to the spontaneous a polarization. They therefore considered only the c_{a1} term and set $c_{a2} = c_{a3} = 0$. We will assume that this can be done for nonzero applied fields as well. The resulting simplified expression for P_a , and the corresponding expression for P_b can be substituted into Eq. (2) to obtain the free energy F_e in terms of the displacements and fields alone. The result is

$$F_e = E_a' \sum_l (-1)^l v_l (w_{l+1} - w_{l-1}) - \frac{1}{2} \frac{c_{a1}'^2}{m} \left[\sum_l (-1)^l v_l (w_{l+1} - w_{l-1}) \right]^2 + E_b' \sum_l w_l - \frac{1}{2} \frac{c_b'^2}{m} \left[\sum_l w_l \right]^2. \quad (3)$$

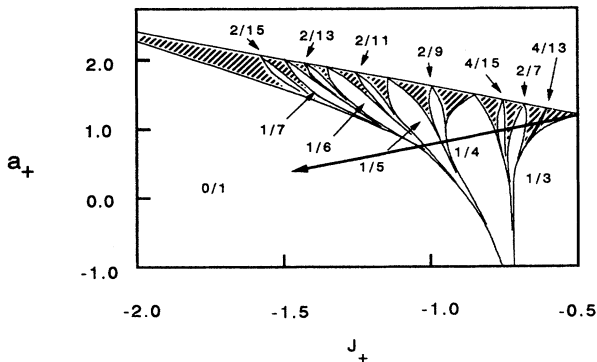


FIG. 1. This is the zero field (J_+, a_+) phase diagram calculated in Ref. 4 with $a_- = 0.4$, $J_- = 0$, and $b = 3$. The low-order commensurate phases have been labeled by their value of α . The shaded regions correspond to higher-order commensurate phases and/or incommensurate phases. The trajectory shown approximately reproduces the succession of wave vectors seen in experiment and their temperature-stability intervals.

Terms involving the fields alone are dropped since they can be assumed fixed at some applied value. The parameters have been scaled for simplification. For example, E_a' has been substituted for $c_{a1} \chi_{0a} E_a$ and c_{a1}' for $c_{a1} / \sqrt{\chi_{0a}}$. Similar remarks apply to E_b' and c_b' .

The equilibrium displacements v_l and w_l in an applied field will be those which minimize the total free energy $F_0 + F_e$. They will now therefore depend on seven parameters—the five originally occurring in F_0 and the c_{a1}' and c_b' of Eq. (3). Note that the c_{a1}' and c_b' terms may contribute to the total free energy even if there are no applied fields. These terms were not considered in Ref. 4 because they couple the displacements of layers arbitrarily far apart. Their introduction here means that the stable states in zero field associated with the free energies F_0 and $F_0 + F_e$ will, in general, be different. However, since F_0 alone was able to successfully reproduce the wave-vector sequence of BCCD, we will set $c_{a1}' = c_b' = 0.001$. This renders the effect of these additional terms small and enables us to set $a_- = 0.4$, $J_- = 0$,

$b=3$, and $a_+=0.8J_++1.6$ as in Ref. 4. We will show that this choice of parameter values is consistent with the stable states and polarizations seen in BCCD when an electric field is applied along its b direction. It is not our intent to suggest, however, that this choice is uniquely able to explain the response of BCCD to an electric field. There may be other sets of values which do equally well or better.

The free energy F_0+F_e can be used to calculate the phase diagram of BCCD in either an applied E'_a or E'_b . Only the E'_b diagram is given here because few experiments have measured the effect of an E'_a field on BCCD. The phase at a given point (J_+, E'_b) in the diagram is characterized by the periodicity of its displacements. These can be determined by extending the numerical methods used to minimize F_0 in Ref. 10. This procedure determines the best displacements with periodicity $\alpha=n/m$. In our case, this is done for all ratios n/m with $m \leq 26$. The displacements which yields the overall minimum determine the stable state.

Figure 2 shows that the stability of states n/m with n even and m odd is favored by the application of a field while for the others it is progressively diminished. These states are known to exhibit a spontaneous b polarization. In this case, Eq. (2) implies that they have $P_b \propto \sum_l w_l \neq 0$ for $E'_b=0$. The third term on the right-hand side of Eq. (3) then gives a contribution to the free energy linear in E'_b . The field will always favor the domain that makes this contribution negative. For the other states, the leading term is, at most, quadratic in E'_b . The lowest-order effect of E'_b is therefore to always favor the spontaneously polar states.

Figure 2 can be compared with the phase diagram of Kopperpieper *et al.*¹¹ They have determined the regions of stability of the $\frac{0}{1}$, $\frac{1}{5}$, $\frac{2}{9}$, $\frac{1}{4}$, and $\frac{2}{7}$ states. Their phase boundaries are in rough agreement with those seen in Fig. 2. Our phase diagram, however, shows additional higher-order phases. Their existence is verified by hysteresis loop measurements that plot P_b against E_b for some fixed temperature. This corresponds, in our diagram, to the polarizations one would encounter by start-

ing off at a particular J_+ and going in the E'_b direction. The steplike behavior seen in the loops can be compared with the discontinuities in the polarization to be expected when crossing first-order lines in our phase diagram. These discontinuities can be evaluated using the expression for P_b in terms of E'_b and w_l that, as previously discussed, can be obtained from Eq. (2). The results are shown in Figs. 3 and 4. The five plots of Fig. 3 can be compared with the ten loops measured by Inruh *et al.*¹ between 117 K (an incommensurate region between $\frac{7}{26}$ and $\frac{4}{15}$) and 115 K (the upper limit of stability of the $\frac{1}{4}$ state). Our $J_+=-0.767$ plot corresponds to their first loop at 116.8 K. Both have an $E_b=0$ phase which is nonpolar and a discontinuity in P_b associated with a field-induced transition to the $\frac{4}{15}$ state. Unruh *et al.*¹ then give several loops showing the movement of the discontinuity to smaller field values as the stability interval of the $\frac{4}{15}$ state is approached. This behavior would be reproduced by our diagram. The plot at $J_+=-0.775$ shows the spontaneous polarization of the $\frac{4}{15}$ state. One encounters a nonpolar state below $\frac{4}{15}$ and the $\frac{4}{15}$ discontinuity again moves off to larger fields. This is shown for $J_+=-0.782$. The remaining two loops of Unruh *et al.*¹ are taken from the polar $\frac{6}{23}$ and nonpolar $\frac{1}{4}$ states. The response of their polarizations to an applied field is well reproduced by our $J_+=-0.786$ and -0.788 plots, respectively.

Rother *et al.*¹² have measured another set of hysteresis loops at 12 different temperatures. Their loops at 124.1, 116.6, 77.1, 75.0, 59.0, and 50.5 K may be compared with ours at $J_+=-0.72$, -0.761 , -0.924 , -0.95 , -0.99 , and -1.032 , respectively. The overall agreement is quite good. We have, however, discontinuities arising from transitions to the $\frac{7}{26}$, $\frac{4}{15}$, and $\frac{5}{18}$ phases in our $J_+=-0.761$ plot not seen in their loop at 116.6 K. It is possible that a more sensitive measurement would have seen these additional discontinuities. It is also possible that Fig. 2 overestimates the stability of these states. If this region of the phase diagram was incommensurate, the wave vector would vary continuously with E_b and

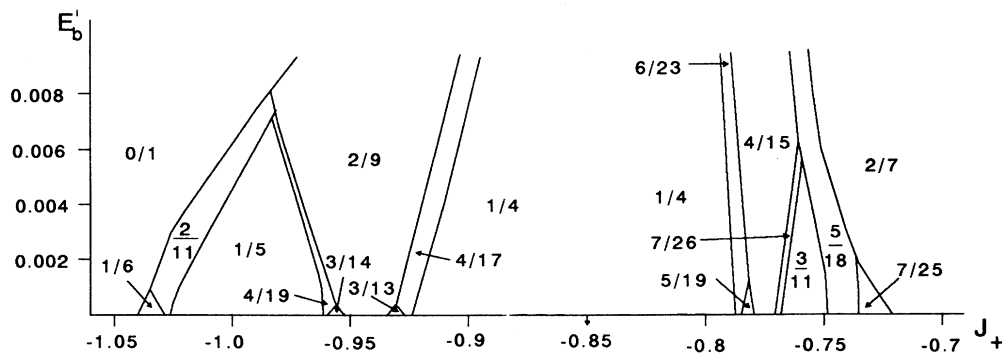


FIG. 2. Our calculated phase diagram of BCCD in an applied E'_b field. The phases have been labeled by their value of $\alpha=n/m$ and only those with $m \leq 26$ have been considered. The $E'_b=0.0$ axis corresponds to the trajectory shown in Fig. 1.

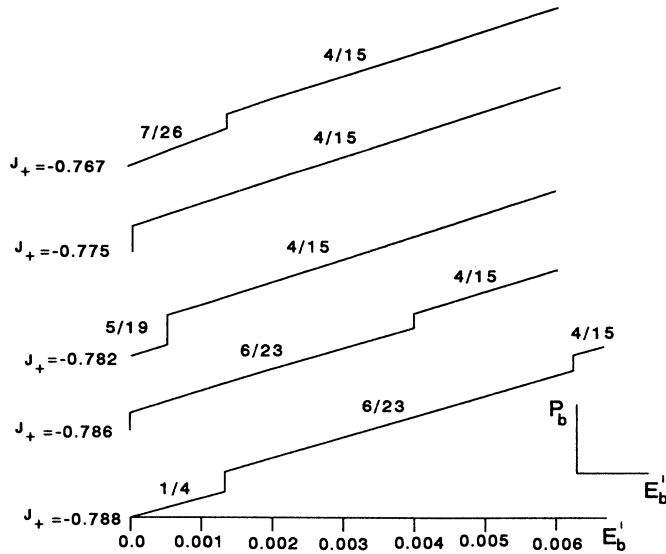


FIG. 3. Plots of P_b vs E'_b for various values of J_+ (temperature). The starting $E'_b=0$ point of each plot is taken as the origin of the vertical P_b axis, so that spontaneously polar states such as $\frac{4}{15}$ and $\frac{6}{23}$ have a jump at $E'_b=0$. The phases associated with each plot have been labeled by α .

there would be no discontinuities in the polarization. Modifying our numerical procedure to deal with incommensurate states may resolve this discrepancy. The 77.1-K loop of Rother *et al.*¹² has a zero-field discontinuity in the polarization. This is explained by our $J_+ = -0.924$ loop as due to the existence of the spontaneously polar $\frac{4}{17}$ state, though it is apparently not known to be stable at zero field. The lower-temperature hysteresis loop measurements seem to indicate that the $\frac{2}{13}$ state occupies a region of stability between the $\frac{2}{11}$ and $\frac{0}{1}$ phases. Its absence in our diagram is probably because, as explained in Ref. 4, our trajectory underestimates a_+ in this temperature region. In conclusion, we note that our previously introduced competing interaction model is consistent with the stable states and polarizations which

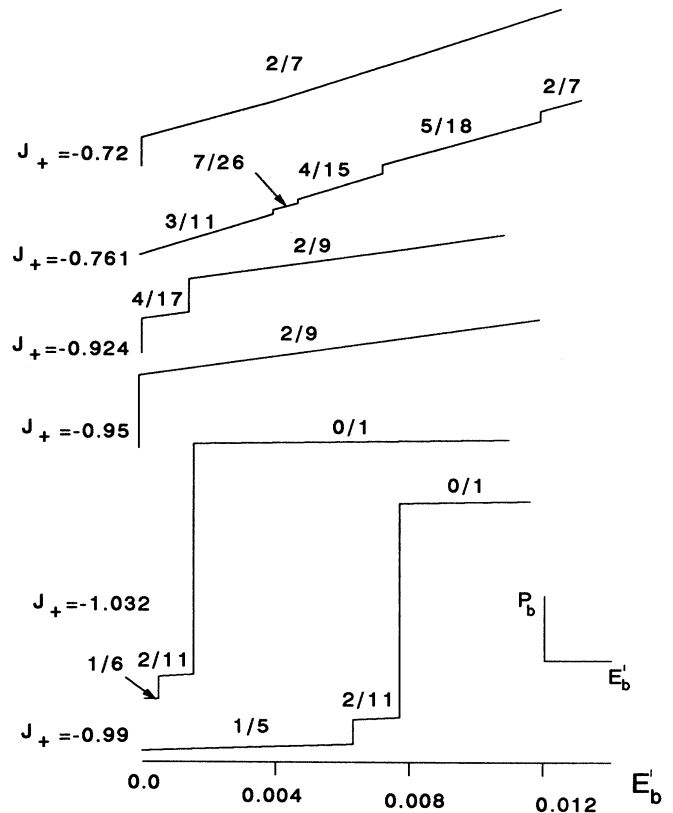


FIG. 4. Plots of P_b vs E'_b . The vertical P_b scales of the $J_+ = -0.99$, -1.032 and $J_+ = -0.924$, -0.95 plots are ten and two times larger, respectively, than the scale of the $J_+ = -0.72$, -0.761 plots.

arise when an electric field is applied along the b direction of BCCD.

This research was supported by the Natural Sciences and Engineering Research Council of Canada. One of us (I.F.) would like to thank the Walter C. Sumner Foundation for financial support.

¹H. G. Unruh, F. Hero, and V. Dvořák, *Solid State Commun.* **70**, 403 (1989).

²W. Brill and K. H. Ehses, *Jpn. J. Appl. Phys.* **24**, 826 (1985).

³J. L. Ribeiro, M. R. Chaves, A. Almeida, J. Albers, A. Klöpperpieper, and H. E. Müser, *J. Phys. Condens. Matter* **1**, 8011 (1989).

⁴Z. Y. Chen and M. B. Walker, *Phys. Rev. B* **43**, 760 (1991).

⁵V. Dvořák, J. Holakovský, and J. Petzelt, *Ferroelectrics* **79**, 15 (1988).

⁶J. L. Ribero, J. C. Tolédano, M. R. Chaves, A. Almeida, H. E. Müser, J. Albers, and A. Klöpperpieper, *Phys. Rev. B* **41**, 2343

(1990).

⁷R. Siems and T. Tentrup, *Ferroelectrics* **98**, 303 (1989).

⁸W. Brill, W. Schildkamp, and J. Spilker, *Z. Kristallogr.* **172**, 281 (1985).

⁹R. Currat, J. F. Legrand, S. Kamba, J. Petzelt, V. Dvořák, and J. Albers, *Solid State Commun.* **75**, 545 (1990).

¹⁰Z. Y. Chen and M. B. Walker, *Phys. Rev. B* **43**, 760 (1991).

¹¹A. Klöpperpieper, H. J. Rother, J. Albers, and H. E. Müser, *Jpn. J. Appl. Phys.* **24**, 829 (1985).

¹²H. J. Rother, J. Albers, and A. Klöpperpieper, *Ferroelectrics* **54**, 107 (1984).